Analytical Biochemistry 410 (2011) 185–190

Contents lists available at ScienceDirect

Analytical Biochemistry

journal homepage: www.elsevier.com/locate/yabio

Mycotoxin detection on antibody-immobilized conducting polymer-supported electrochemically polymerized acacia gum

Raju Khan [a], Nibaran C. Dey [a], Ajit K. Hazarika [a], Krishan K. Saini [b], Marshal Dhayal [c,*]

[a] Analytical Chemistry Division, North East Institute of Science & Technology, Jorhat 785006, Assam, India
[b] Engineering Materials Division, National Physical Laboratory, New Delhi 110012, India
[c] Centre for Cellular and Molecular Biology, Hyderabad 500007, India

ARTICLE INFO

Article history:
Received 12 July 2010
Received in revised form 1 November 2010
Accepted 4 November 2010
Available online 13 November 2010

Keywords:
Polyaniline
Acacia gum
Immunosensor
Electrochemical impedance spectroscopy

ABSTRACT

Electrochemical polymerization of acacia gum (AG) was initiated by electroactive polyaniline (PANI) monomers by radical cation formation and their coupling reactions with AG molecules. R_{CT} values obtained from electrochemical impedance spectroscopy analysis at various AG concentrations with PANI were drastically decreased, confirming formation of conducting AG complexes with PANI. Quantitative analysis of ochratoxin-A (OTA) detection in electrolyte was carried out on rabbit antibody-immobilized PANI and PANI–AG matrices. The observed sensitivities of 50, 150, and 250 mg AG-added PANI matrix-based platforms were 3.3 ± 0.5, 10.0 ± 0.5, and 12.7 ± 0.5 μA/ng/ml, respectively. The sensitivity of only PANI electrodes was 2.6 ± 0.3 μA/ng/ml, which was relatively lower than AG-added PANI. This increase was due to the presence of glycan functional groups in AG molecules that supported the retention of activity of antibodies. In addition, enhanced electron transportation at AG–PANI film surface was observed due to formation of an electroactive polymer film of two different electroactive functions to contribute toward enhancement in the detection sensitivity.

To determine the function of biomolecules for biosensor applications, several methods have been used, including high-performance liquid chromatography (HPLC)[1] [1], thin layer chromatography (TLC) [2], enzyme-linked immunosorbent assay (ELISA) [3], and electrochemical immunoassay [4–6]. During recent years, several researcher groups [7,8] have been devoted to the development of biomaterials that allow the detection of toxic compounds at very low concentrations of mycotoxins found in food products such as cereal grains, vegetables and dried fruit, meat, and fish. For such applications, an electrochemical immunosensor [9] based on new functional biomaterial can have great potential toward detection of mycotoxins at low cost and higher sensitivity by enhancing orientation of electrode-bound antibodies [3]. Due to unique structural and functional characteristics, the organically synthesized glycans are considered as the most preferred biomaterials for biomedical applications [10–13].

The organic synthetic processes [14] for glycans are very complex; therefore, exploring the usability of naturally existing glycans for stable thin film formation can be an interesting choice toward development of functional biomaterials for such applications. For example, acacia gum (AG, gum arabic) is a complicated mixture of long and short chains of arabinogalactan oligosaccharides, polysaccharides, and glycoproteins. Gum arabic consists of a mixture of lower molecular weight polysaccharide (MW $\sim 0.25 \times 10^6$, major component) and higher molecular weight hydroxyproline-rich glycoprotein (MW $\sim 2.5 \times 10^6$, minor component) [15,16]. In the past, this has been used as the glue on stamps and as a flavor stabilizer in soft drinks [17]. The chemical and physical properties of AG as a bulk material (not for stable thin film formation) has been very well studied, and variations in functionalities of AG corresponding to polymers, oxides, and proteins have been established [18–20].

In the current study, our objective was to establish a method for electrochemical polymerization of AG–polyaniline (PANI) toward development of functional biopolymer-based biodegradable conducting platforms that are suitable for application in biosensors. The presence of unique compositions of carbohydrates and glycoproteins in AG can support biocompatibility [21,22] of these platforms for biomedical applications; conducting characteristics of biopolymer matrices encourage further exploration of this. We should note that only AG (without PANI) thin films cannot be obtained by electrochemical polymerization. Adding PANI to AG can

* Corresponding author. Fax: +91 040 271 60591.
E-mail addresses: marshal@ccmb.res.in, marshaldhayal@yahoo.com (M. Dhayal).

[1] *Abbreviations used:* HPLC, high-performance liquid chromatography; TLC, thin layer chromatography; ELISA, enzyme-linked immunosorbent assay; AG, acacia gum (gum arabic); PANI, polyaniline; FT-IR, Fourier transform infrared; OTA, ochratoxin-A; SPR, surface plasmon resonance; MIPPy, molecularly imprinted polypyrrole; IgG, immunoglobulin G; PBS, phosphate buffer solution; ITO, indium tin oxide; BSA, bovine serum albumin; CV, cyclic voltammetry; EIS, electrochemical impedance spectroscopy; DPV, differential pulse voltammetry; SEM, scanning electron microscopy.

0003-2697/$ - see front matter © 2010 Elsevier Inc. All rights reserved.
doi:10.1016/j.ab.2010.11.013

provide us with an opportunity to develop bioactive functional films.

PANI–AG films have been characterized by different techniques such as scanning electron microscopy, Fourier transform infrared (FT-IR) spectroscopy, and electrochemical characterization, and their usefulness for an immunosensor has been discussed for the detection of ochratoxin-A (OTA). OTA is one of the most abundant food-contaminating mycotoxins produced by some species of *Penicillium chrysogenum* and *Aspergillus carbonarius* [23,24]. Previously, Yu and Lai [25] used a miniaturized surface plasmon resonance (SPR) device for detection of OTA with molecularly imprinted polypyrrole (MIPPy) film deposited by electrochemical polymerization from a solution of pyrrole and OTA. They correlated increases in SPR angle with in situ film growth, and binding properties of the MIPPy film were investigated by loading OTA standard solutions into the integrated SPR flow cell. In the current study, we report a simple approach where natural glycans (AG) can be electrochemically polymerized onto a conducting substrate that can subsequently be used as a platform for immobilization of immunoglobulin Gs (IgGs) to detect OTA based on IgG–OTA interaction in electrolyte.

Materials and methods

Materials

AG (99%), aniline (99.5%), and hydrochloric acid (32%) of analytical grade were purchased from Sigma–Aldrich. OTA from *Aspergillus ochraceus* (*Aspergillus oryzae*) was purchased from Sigma–Aldrich, and OTA solution was prepared by dissolving in phosphate buffer solution (PBS) with 10% methanol.

Thin film formation

Polymerization of aniline on ITO (indium tin oxide) electrode was carried out by electrochemical methods by applying an appropriate oxidation potential [26]. We used the chronoamperometry technique for the film formation by adjusting the potential at −0.2 to 0.9 mV in 150 s from solutions containing 0.2 M aniline into 1 M HCl solution prepared in 10 ml of deionized water. Aniline in electrolyte was added to support electrochemical polymerization of AG at different weight percentages (50–250 mg in 0.2 M aniline-based 1 M HCl solution). The active electrode surface area for biosensor was 0.25 cm^2, which was controlled by placing a physical mask during thin film formation.

Antibody immobilization

Rabbit antibody (IgG) solution was prepared in 50 mM PBS at pH 7.4, and 0.15 M NaN_3 was used as a preservative. Freshly prepared 10 μl of IgG solution was spread on PANI, AG, and PANI–AG electrodes and then incubated at 4 °C for 12 h. The IgG-immobilized electrodes were washed with PBS to remove unbounded sites. Bovine serum albumin (BSA, 98% purity) dissolved in PBS was immobilized for 6 h at 4 °C to prevent nonspecific interactions of mycotoxins at the surface.

Surface characterization

Thin films were characterized using FT-IR spectra recorded on a PerkinElmer spectrophotometer, and Autolab cyclic voltammetry (CV) equipment (Autolab 302N model) was used for electrochemical characterization of biosensors with a three-electrode system. All electrochemical impedance spectroscopy (EIS) measurements were carried out at a constant temperature in the frequency range of 0.01 to 10^5 Hz with a peak-to-peak excursion of 5 mV superimposed on a 250-mV initial potential using PBS (50 mM [pH 7.0] and 0.9% NaCl) containing $Fe[(CN)_6]^{3/4-}$ as electrolyte. The CV cell was fitted with platinum wire and Ag/AgCl as counter and reference electrodes, respectively.

Results and discussion

FT-IR spectra of electrochemical polymerized PANI and AG-added PANI films were obtained to characterize the chemical interactions between PANI and AG. FT-IR spectra of PANI have a strong absorption band between 714 and 843 cm^{-1} due to both the presence of an aromatic ring and deformation of C—H vibrations, as shown in Fig. 1A. In the spectra, bands between 1204 and 1343 cm^{-1} were associated with C—N stretching in aromatic amines and 1648 cm^{-1} due to C=C stretching of benzenoid rings and quinoid rings. The strong peak at 2355 cm^{-1} was associated

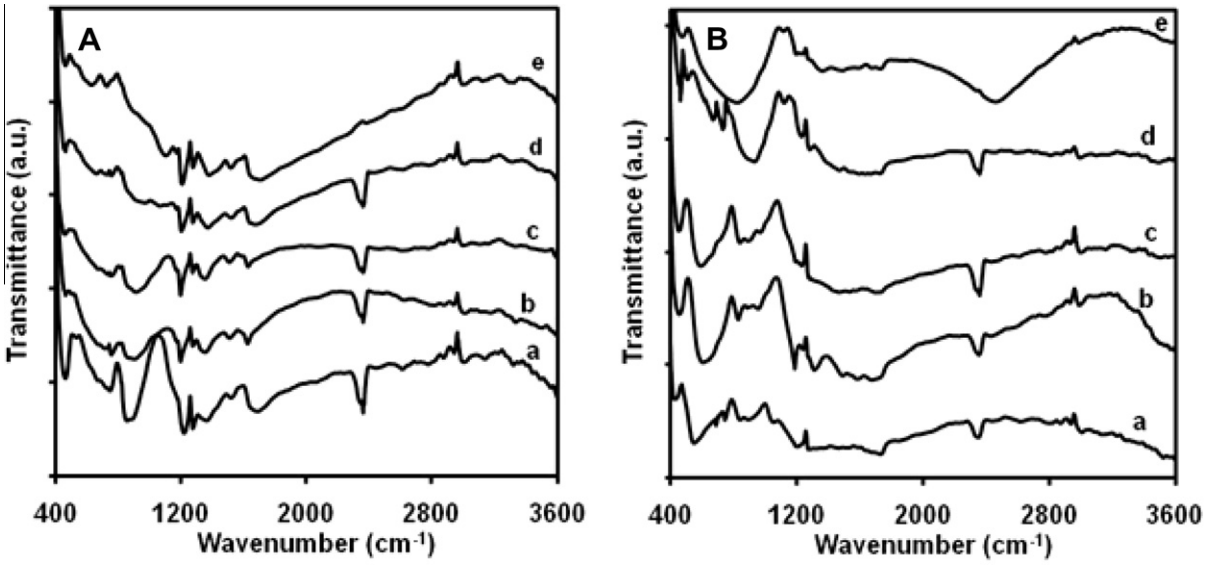

Fig.1. (A) FT-IR spectra of PANI (a) and PANI–AG matrices at different masses of AG in PANI: (b) 50 mg; (c) 150 mg; (d) 250 mg; (e) 350 mg. (B) FT-IR spectra of rabbit antibody-immobilized PANI (a) and PANI–AG matrices at different masses of AG in PANI: (b) 50 mg; (c) 150 mg; (d) 250 mg; (e) 350 mg.

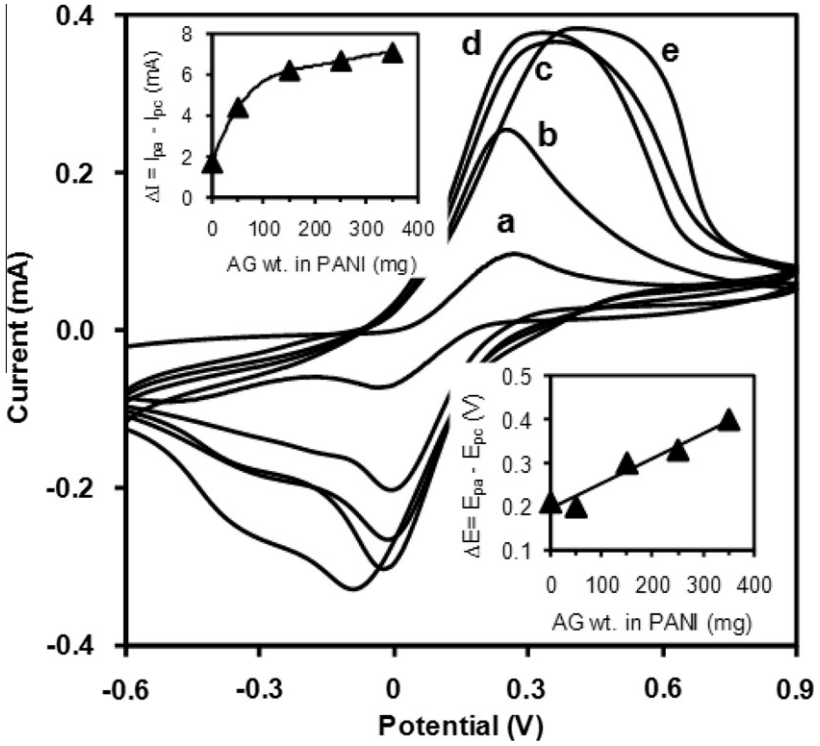

Fig.2. CV measurements of PANI (a) and PANI–AG matrices at different masses of AG in PANI: (b) 50 mg; (c) 150 mg; (d) 250 mg; (e) 350 mg.

with –N≡N in diazonium salts. The IR band at 2982 to 3300 cm^{-1} corresponds to N—H stretching with hydrogen-bonded amino groups and free O—H stretching vibration. At all concentrations of AG-added PANI thin film, FT-IR spectra have a sharp peak at 745 cm^{-1} that could be due to the presence of an aromatic ring and possible deformation of C–H vibrations in PANI. Two distinct broadenings observed between 500 to 694 cm^{-1} and 835 to 975 cm^{-1} confirmed strong binding of AG molecules with PANI [18]. The relative increase in proportion of AG concentration in PANI had increased broadening of these peaks from 474 to 733 cm^{-1} and from 780 to 1132 cm^{-1}. The distinct peak associated with AG at 745 cm^{-1} was also merged in the PANI–AG matrix, confirming AG binding with PANI molecules.

Antibodies were immobilized on these electrodes and FT-IR spectra of IgG-immobilized electrodes were observed, confirming successful immobilization of antibodies (Fig. 1B). Absorption peaks from 1699 to 1456 cm^{-1} were associated with the presence of amide I and II groups of the antibody on the surface [27]. A significant decrease in intensity of the bands between 1286 and 1179 cm^{-1} was observed. These observations give a strong indication of IgGs binding with matrix molecules at PANI–AG thin film surfaces.

CV measurements were performed to characterize the PANI and AG–PANI films developed by electrochemical polymerization on the conducting electrodes and are shown in Fig. 2. Different AG weight percentage-added PANI deposited electrodes were immersed in PBS (50 mM [pH 7.4] and 0.9% NaCl) containing $Fe[(CN)_6]^{3/4-}$ and recorded at a constant scan rate of 30 mV s^{-1}. The only PANI thin film deposited electrode was also characterized under the same conditions to investigate effects of AG. The redox current peaks centered roughly at 0.23 V in CV of PANI shifted toward higher potentials, indicating that reduction in kinetic constants and their peak heights increased when the concentration of AG was increased. On the addition of AG in PANI, the CV observation indicates a new redox process that appeared at higher potentials, indicating the formation of an electroactive polymer film of two different compounds. This additional redox peak broadened the peak observed in AG-added PANI films. These observations suggest that the polymerization of AG was initiated by electroactive aniline monomers by radical cation formation and their coupling reactions with AG molecules. The difference between cathodic peak (E_{pc}) and anodic peak (E_{pa}) shift ($\Delta E_p = E_{pa} - E_{pc}$) was evaluated to determine the kinetics of electron transfer in these matrices [28]. Similarly, a relative increase in current was observed due to the fast redox process at the PANI–AG matrix surface relative to only PANI.

CV measurements were carried out on IgG-immobilized film surfaces in PBS (50 mM [pH 7.4] and 0.9% NaCl) containing $Fe[(CN)_6]^{3/4-}$ and were recorded at a constant scan rate of 30 mV s^{-1} (Fig. 3). A relative decrease in the reduction current was observed, also confirming immobilization of IgGs on these surfaces. A decrease in broadening of peaks indicates the binding of IgGs with AG molecules or the possibility of diffusion prevention by IgGs that could have occupied porous spaces available at electrode surfaces.

The hybrid PANI–AG matrices were also characterized using differential pulse voltammetry (DPV) measurements with varying potential scans from −0.2 to +0.4 V and are shown in Fig. 4. The first-derivative voltammograms corresponding to the differential pulse voltammograms also were obtained to estimate anodic peak potentials of hybrid PANI–AG matrices by getting an intercept at zero. DPV is a very useful technique for measuring trace levels of organic and inorganic species in which the height of the measured current is directly proportional to the concentration of the corresponding analytes. In the observed current–voltage response, the peak potential (E_p) can be used to identify the species as $E_p = E_{1/2} - \Delta E/2$, where $E_{1/2}$ is the polarographic half-wave potential and ΔE is the pulse amplitude used in the DPV measurements. Observations indicate that the addition of AG in PANI increased the current corresponding to the peak potential as compared with

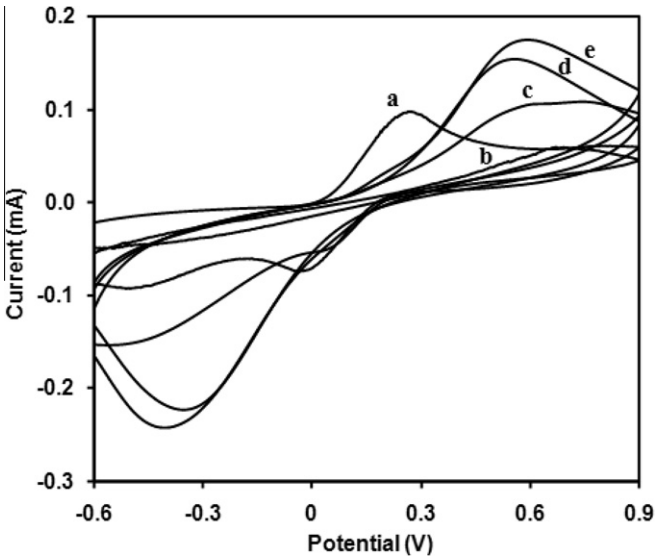

Fig.3. CV measurements of BSA-backfilled IgG-immobilized PANI (a) and PANI–AG matrices at different masses of AG in PANI: (b) 50 mg; (c) 150 mg; (d) 250 mg; (e) 350 mg.

that in PANI films. In addition to an increase in current at higher potentials, an additional peak indicates incorporation of AG with PANI in the film. The distinct peak that corresponds to AG shifted toward the lower peak potential with increasing proportions of AG in PANI. The process resulted in broadening of spectra, and an increase in peak current was consistent with CV measurements discussed above.

PANI and PANI–AG (at three different concentrations [50, 150, and 250 mg] of AG in PANI, with data for 350 mg AG in PANI now shown) film surface morphology was observed using scanning electron microscopy (SEM) and are shown in Fig. 5. SEM observations show very good uniformity, and the addition of AG in PANI improved both the uniformity and porosity in PANI–AG films. The contact angle of films at different concentrations of AG in PANI and only PANI were obtained (see Fig. 1 in Supplementary Material). The initial increase in AG concentration in PANI increased the hydrophobic characteristics of the films, and it reached saturation for films prepared from 150 mg wt% AG added in 0.2 M aniline-based 1 M HCl solution. Further increases in AG weight percentage decreased the hydrophobic nature of films relative to only PANI. This relative change in contact angle can be associated with per unit area adhesion energy, which can be controlled by both surface morphology and surface chemistry of film surfaces.

To investigate the effect of surface charge modulation to determine relative change in surface charge resistance at zero potential on PANI and AG-added PANI films deposited electrode surface, EIS response was observed (Fig. 6). The Nyquist plot of impedance was obtained from real (Z') and imaginary (Z'') impedance at different frequencies to determine charge transfer kinetics of different weight percentage AG-added PANI films and was compared with only PANI. Interfacial R_{CT} and C_d in the Nyquist plot of impedance were obtained from real (Z') and imaginary ($-Z''$) impedance at different frequencies for a parallel RC circuit and are shown in Table 1. The R_{CT} value of PANI–AG was drastically decreased and indicated that AG binding with PANI supported charge transfer at the electrode interface. Warburg resistance (Z_w) of thin film surfaces also was calculated from the Nyquist plot shown in Fig. 6. This was associated with an intercept of the straight line, which had a slope of unity that was derived from $Z_w(\omega) = W_{int} + (R_p\lambda/\sqrt{2}\omega)[1 - j]$ and $W_{int} = R_s + R_p - R_p^2\lambda^2 C_d$, where $\lambda = (k_f/\sqrt{D_O} + k_b/\sqrt{D_R})$, k_f and k_b are forward and backward electron transfer rate constants, respectively, and D_O and D_R are the oxidant and reductant diffusion coefficients, respectively. Electrolyte solution resistance (R_s), polarization resistance (R_p), and λ values are listed in Table 1. These observations indicate significant Warburg resistance [28] (R_w) at low frequencies. Relative changes in oxidant and reductant diffusion coefficients can be seen with observed variations in the intercept of straight line (associated with Warburg resistance) from the Nyquist plot shown in Fig. 6. R_s and $R_s + R_{CT}$ values were obtained from standard commercial software available with the instrument and were also calculated separately from the semicircle and straight line fitting in the Excel spreadsheet. Both observations have shown very good agreement with values obtained in this study.

DPV was used to obtain current–voltage characteristics of PANI–AG matrices at different concentrations of OTA in electrolyte, and the relative change in peak current was recorded. OTA detection was carried out by placing IgG-immobilized working

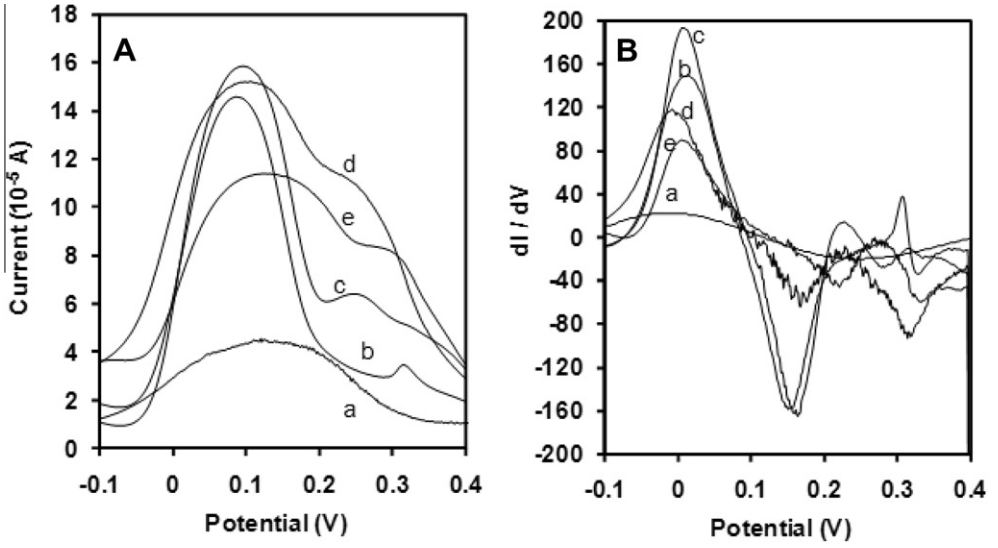

Fig.4. (A) DPV measurements of PANI (a), PANI–AG matrix at 50 mg mass of AG in PANI (b), PANI–AG matrix at 150 mg mass of AG in PANI (c), PANI–AG matrix at 250 mg mass of AG in PANI (d), and PANI–AG matrix at 350 mg mass of AG in PANI (e). (B) Corresponding first-derivative DPV measurements.

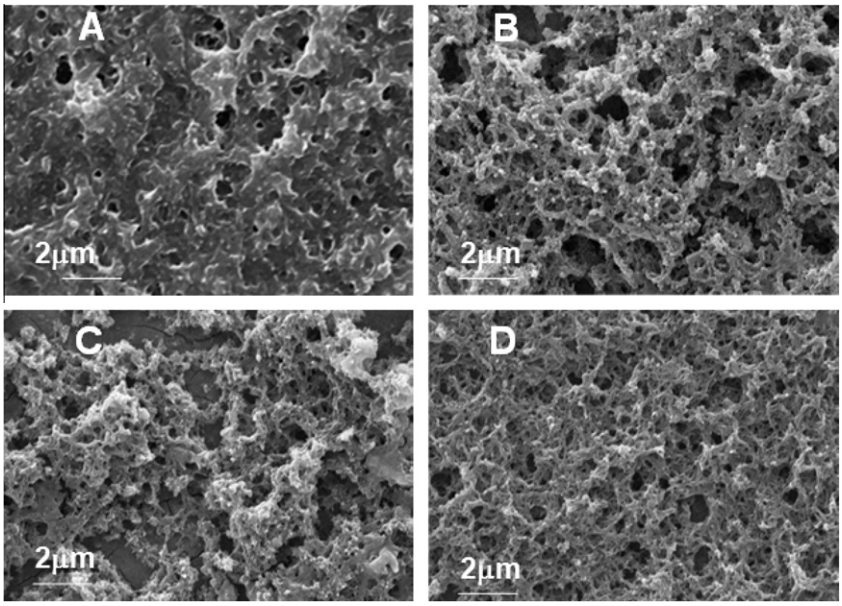

Fig.5. SEM pictures of PANI (A) and PANI–AG matrices at different masses of AG in PANI: (B) 50 mg; (C) 150 mg; (D) 250 mg.

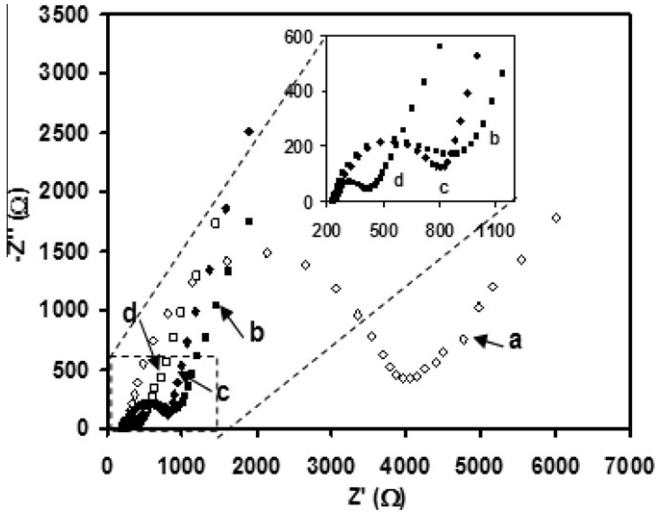

Fig.6. Nyquist plot of PANI (a) and PANI–AG matrices at different masses of AG in PANI: (b) 50 mg; (c) 150 mg; (d) 250 mg.

Table 1
Electrolyte solution resistance (R_s), polarization resistance (R_p), and λ values at four different conditions: PANI (a) and PANI–AG matrices at different masses of AG in PANI: (b) 50 mg, (c) 150 mg, and (d) 250 mg.

Matrix	R_s (Ω)	R_p (Ω)	C_d (μF)	λ	ϕ
a	634	3689	0.73	7.096	−39.0
b	245	606	6.80	5.530	−24.6
c	227	664	4.10	4.412	−25.7
d	228	200	2.60	17.710	−13.3

electrodes in 10 ml of phosphate buffer (50 mM [pH 7.0] and 0.9% NaCl) containing $Fe[(CN)_6]^{3/4-}$. DVP measurements were carried out after adding 20 μl of OTA stock solution, which contains 5 ng of OTA concentration, to 10 ml of buffer solution. The solution was stirred for 30 s before taking each DPV measurement. The OTA concentration was increased by adding 20 μl of OTA stock solution with gradual increments in buffer solution. Platinum wire and Ag/AgCl were used as counter and reference electrodes, respectively. The relative change in peak current for only PANI was very small, possibly due to the low level of IgG immobilization on its surfaces.

Fig. 7 shows quantitative analysis of OTA detection in terms of relative changes in peak current (ΔI_{SC}) for PANI–AG matrices. Where $\Delta I_p = I_{p,x} - I_{p,0}$, $I_{p,0}$ was the peak current without OTA and $I_{p,x}$ was the peak current for a particular concentration of OTA in electrolyte. The linear response for detection of OTA was strongly dependent on the amount of AG added in PANI. OTA detection sensitivity was calculated from the slope of the linear response in current variation with increasing OTA concentrations. Sensitivities of 50, 150, and 250 mg AG-added PANI matrix-based immunosensor were calculated from the corresponding linear responses between 0.5 ng/ml (lower limit) and 3 ng/ml (higher limit) OTA concentrations in electrolyte.

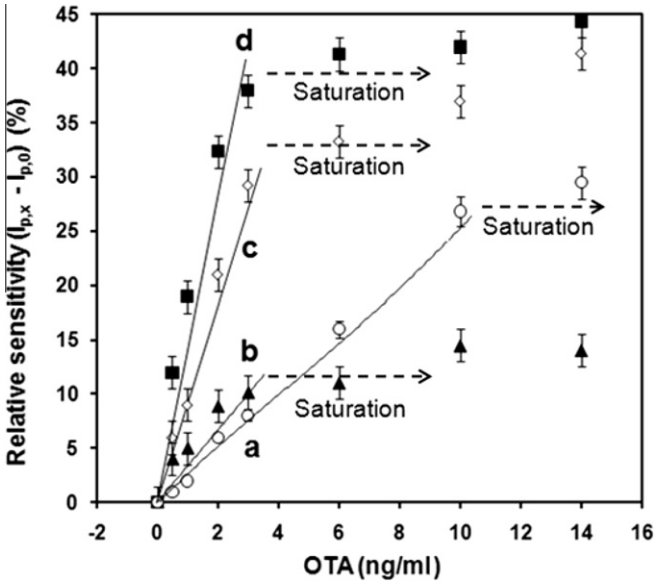

Fig.7. Linear response with OTA detection on PANI (a) and PANI–AG matrices at different masses of AG in PANI: (b) 50 mg; (c) 150 mg; (d) 250 mg.

The observed sensitivities of 50, 150, and 250 mg AG-added PANI matrix-based platforms were 3.3 ± 0.5, 10.0 ± 0.5, and 12.7 ± 0.5 μA/ng/ml. The sensitivity of only PANI electrodes was 2.6 ± 0.3 μA/ng/ml, which was lower than that of AG-added PANI. The observed relative variations in OTA detection sensitivity corresponded to enhanced electrochemical responses of AG-added PANI films shown in Figs. 4 and 6. This increase was possibly due to the presence of glycan functional groups in AG molecules supporting the retention of activity of IgGs immobilized. In addition, these surfaces increased the capability of enhancing electron transportation at the AG–PANI film surface due to formation of an electroactive polymer film of two different electroactive functions that also supports the enhancement in the detection sensitivity. Previously, Alarcon and coworkers [29] used electrochemical ELISA for the quantitative determination of OTA using polyclonal antibodies on carbon-based screen-printed electrodes. The detection sensitivity was 6.1 ± 0.1 ng ml^{-1}, and in our case it increased more than two times on AG-added PANI electrodes.

Conclusions

The electrochemical polymerization process for stable thin film deposition of AG with PANI has been described. AG molecules in PANI have enhanced charge transfer and current–voltage characteristics at the electrode interface. Increases in oxidation peak current and enhanced broadening were observed due to the fast redox process in the PANI–AG matrix. Optical and electrochemical measurements confirmed successive IgG immobilization on the PANI–AG surface. The relative proportion of AG in PANI was optimized to characterize the linear response of the immunosensor to detect toxic compounds in electrolyte. The observed sensitivities of 50, 150, and 250 mg AG-added PANI matrix-based platforms were 3.3 ± 0.5, 10.0 ± 0.5, and 12.7 ± 0.5 μA/ng/ml, respectively. The sensitivity of only PANI electrodes was 2.6 ± 0.3 μA/ng/ml, which was lower than that of AG-added PANI.

Acknowledgments

Raju Khan thanks the Department of Science & Technology (DST), Government of India, for financial support under the Young Scientist project (SR/FTP/CS-77/2007). Marshal Dhayal is grateful for financial support from the Department of Biotechnology, Government of India, and the director (Dr. Ch Mohan Rao) of the CCMB. The authors also thank Dr. Shashi Singh (CCMB) for reading this manuscript and giving useful feedback.

Appendix A. Supplementary data

Supplementary data associated with this article can be found, in the online version, at doi:10.1016/j.ab.2010.11.013.

References

[1] H. Valenta, Chromatographic methods for the determination of ochratoxin A in animal and human tissues and fluids, J. Chromatogr. A 815 (1998) 75–92.
[2] L. Monaci, F. Palmisano, Ochratoxin A detection in foods: state-of-the-art and analytical challenges, Anal. Bioanal. Chem. 378 (2004) 96–103.
[3] S.H. Alarcon, G. Palleschi, D. Compagnone, M. Pascale, A. Visconti, I. Barna-Vetro, Monoclonal antibody based electrochemical immunosensor for the determination of ochratoxin A in wheat, Talanta 69 (2006) 1031–1037.
[4] B. Prieto-Simon, M. Campas, J. Marty, T. Noguer, Novel highly-performing immunosensor-based strategy for ochratoxin A detection in wine samples, Biosens. Bioelectron. 23 (2008) 995–1002.
[5] R. Khan, M. Dhayal, Chitosan/polyaniline hybrid conducting biopolymer base impedimetric immunosensor to detect ochratoxin-A, Biosens. Bioelectron. 24 (2009) 1700–1705.
[6] R. Khan, M. Dhayal, Nanocrystalline bioactive TiO_2–chitosan impedimetric immunosensor for ochratoxin-A, Electrochem. Commun. 10 (2008) 492–495.
[7] A.G. Mantzila, V. Maipa, M.I. Prodromidis, Development of a Faradic impedimetric immunosensor for the detection of *Salmonella typhimurium* in milk, Anal. Chem. 80 (2008) 1169–1175.
[8] P.R.B. de O. Marques, A. Lermo, S. Campoy, H. Yamanaka, J. Barb, S. Alegret, M.I. Pividori, Double-tagging polymerase chain reaction with a thiolated primer and electrochemical genosensing based on gold nanocomposite sensor for food safety, Anal. Chem. 81 (2009) 1332–1339.
[9] Y. Fu, P. Li, L. Bu, T. Wang, Q. Xie, X. Xu, L. Lei, C. Zou, S. Yao, Chemical/biochemical preparation of new polymeric bionanocomposites with enzyme labels immobilized at high load and activity for high-performance electrochemical immunoassay, J. Phys. Chem. C 114 (2010) 1472–1480.
[10] D.P. Chang, N.I. Abu-Lail, F. Guilak, G.D. Jay, S. Zauscher, Conformational mechanics, adsorption, and normal force interactions of lubricin and hyaluronic acid on model surfaces, Langmuir 24 (2008) 1183–1193.
[11] M.R. Pratt, C.R. Bertozzi, Synthetic glycopeptides and glycoproteins as tools for biology and as therapeutic agents, Chem. Soc. Rev. 34 (2005) 58–68.
[12] M.L. Shao, H.J. Bai, H.L. Gou, J.J. Xu, H.Y. Chen, Cytosensing and evaluation of cell surface glycoprotein based on a biocompatible poly(diallydimethylammonium) doped poly(dimethylsiloxane) film, Langmuir (2009) 3089–3095.
[13] M. Metzke, J.Z. Bai, Z. Guan, A novel carbohydrate-derived side-chain polyether with excellent protein resistance, J. Am. Chem. Soc. 125 (2003) 7760–7761.
[14] D.P. Gamblin, E.M. Scanlan, B.G. Davis, Glycoprotein synthesis: an update, Chem. Rev. 109 (2009) 131–163.
[15] L.J. Goodrum, A. Patel, J.F. Leykam, M.J. Kieliszewski, Gum arabic glycoprotein contains glycomodules of both extension and arabinogalactan–glycoproteins, Phytochemistry 54 (2000) 99–106.
[16] D. Renard, L. Lavenant-Gourgeon, M.C. Ralet, C. Sanchez, Acacia senegal gum: continuum of molecular species differing by their protein to sugar ratio, molecular weight, and charges, Biomacromolecules 7 (2006) 2637–2649.
[17] P.A. Williams, G.O. Phillips, Gum arabic, in: G.O. Phillips, P.A. Williams (Eds.), Handbook of Hydrocolloids, CRC Press, Cambridge, UK, 2000, pp. 155–168.
[18] C.A. Amarnath, S. Palaniappan, P. Rannou, A. Pron, Acacia stabilized polyaniline dispersions: preparation, properties, and blending with poly(vinyl alcohol), Thin Solid Films 10 (2008) 2928–2933.
[19] A. Tiwari, A.P. Mishra, S.R. Dhakate, R. Khan, S.K. Shukla, Synthesis of electrically active biopolymer–SiO_2 nanocomposite aerogel, Mater. Lett. 61 (2007) 4587–4590.
[20] C. Sanchez, D. Renard, Stability and structure of protein–polysaccharide coacervates in the presence of protein aggregates, Int. J. Pharm. 242 (2002) 319–324.
[21] G.O. Phillips, T. Ogasawara, K. Ushida, The regulatory and scientific approach to defining gum arabic (acacia senegal and acacia seyal) as a dietary fibre, Food Hydrocolloids 22 (2008) 24–35.
[22] Y. Dror, Y. Cohen, R.Y. Rozen, Structure of gum arabic in aqueous solution, J. Polym. Sci. B 44 (2006) 3265–3271.
[23] K.J. van der Merwe, P.S. Steyn, L. Fourie, D.B. Scott, J.J. Theron, Ochratoxin A, a toxic metabolite produced by *Aspergillus ochraceus* Wilh., Nature 205 (1965) 1112–1113.
[24] I. Losito, L. Monaci, F. Palmisano, G. Tantillo, Determination of ochratoxin A in meat products by high-performance liquid chromatography coupled to electrospray ionisation sequential mass spectrometry, Rapid Commun. Mass Spectrom. 18 (2004) 1965–1971.
[25] J.C.C. Yu, E.P.C. Lai, Interaction of ochratoxin A with molecularly imprinted polypyrrole film on surface plasmon resonance sensor, Reactive Funct. Polym. 63 (2005) 171–176.
[26] Z. Mondic, L. Duic, F. Kocacicek, The influence of counter-ions on nucleation and growth of electrochemically synthesized polyaniline film, Electrochim. Acta 42 (1996) 1389–1402.
[27] S. Dong, G. Luo, J. Feng, Q. Li, H. Gao, Immunoassay of staphylococcal enterotoxin C1 by FTIR spectroscopy and electrochemical gold electrode, Electroanalysis 13 (2001) 30–33.
[28] A.J. Bard, L.R. Faulkner, Electrochemical Methods, John Wiley, New York, 2000.
[29] S.H. Alarcon, L. Micheli, G. Palleschi, D. Compagnone, Development of an electrochemical immunosensor for ochratoxin-A, Anal. Lett. 37 (2004) 1545–1558.